

# In Vitro Evolution of Amphioxus Insulin-like Peptide to Mammalian Insulin<sup>†</sup>

Zhan-Yun Guo, Lu Shen, Wen Gu, An-Zheng Wu, Jian-Guo Ma, and You-Min Feng\*

*Institute of Biochemistry and Cell Biology, Shanghai Institutes for Biological Sciences, Chinese Academy of Sciences, 320 Yue-Yang Road, Shanghai 200031, China*

*Received March 21, 2002; Revised Manuscript Received June 25, 2002*

**ABSTRACT:** By site-directed mutagenesis, six insulin residues related to the insulin–receptor interaction were grafted, partially or fully, onto the corresponding position of a recombinant amphioxus insulin-like peptide (ILP) that contained the A- and B-domains of the deduced amphioxus ILP. After fermentation, purification, and enzymatic cleavage, six insulin-like double-chain ILP analogues were obtained: [A2Ile]-ILP, [B12Val, B16Tyr]ILP, [B25Phe]ILP, [A2Ile, B12Val, B16Tyr, B25Phe]ILP (four-mutated ILP), [A2Ile, B12Val, B16Tyr, B24Phe, B25Phe]ILP (five-mutated ILP), and [A2Ile, B12Val, B16Tyr, B24Phe, B25Phe, B26Tyr]ILP (six-mutated ILP). Circular dichroism analysis showed that such replacement did not significantly affect their secondary and tertiary structure compared with that of the wild-type ILP. The insulin-receptor-binding activity of the four-, five-, and six-mutated ILP was 0.14%, 11%, and 11% of native insulin, respectively; the other three ILP analogues acquired none of the detectable insulin-receptor-binding potency. The growth-promoting activities of the five- and six-mutated ILP were both about 50% of native insulin, while that of the wild-type ILP was not detectable. By structure–function-based mutagenesis, the completely inactive amphioxus ILP was converted into a molecule with moderate mammalian insulin activity. These results indicated the following: first, the grafted as well as those inborn insulin-receptor-binding related residues can form an insulin-receptor-binding patch on the ILP analogues; second, the ILP can be used as a scaffold molecule to investigate the role of the insulin residues; third, the natural evolution of amphioxus ILP to mammalian insulin is a possible process and can be mimicked in the laboratory.

Insulin superfamily includes insulin, IGF-1,<sup>1</sup> IGF-2, relaxin, bombixin, and some other structurally related small globular proteins (1). Among them, insulin and IGF-1 share the most structural and biological similarities, including highly homologous sequence, three identical disulfide linkages, similar three-dimensional structure, weakly overlapping biological activity, and a common ancestor cloned from amphioxus (2–4). The amphioxus insulin-like peptide (ILP) deduced from the cDNA sequence is a polypeptide that displays structural characteristics of both mammalian insulin and IGF-1 (4). The deduced ILP contains B-, C-, A-, and D-domains similar to IGF-1 while there are potential prohormone convertase cleavage sites at the two ends of the C-domain similar to proinsulin, and its A- and B-domains bear considerable sequence homology to the A- and B-chains of insulin as well as to the A- and B-domains of IGF-1. However, the chemically synthesized or expressed double-chain ILP containing the deduced B- and A-domains has

none of the mammalian insulin activity (5, 6). Katsoyannis and co-workers chemically synthesized double-chain ILP-(A)/insulin(B) hybrid (5) as well as its analogues in which some residues of the ILP A-domain were replaced by the corresponding residues of insulin or IGF-1, and the hybrid acquired 5.0% and the analogues acquired equal to or greater insulin activity (7). However, no modifications on the ILP itself or its B-domain have been carried out since the recombination of the separate A- and B-domains of ILP was ineffective and the recombination of the A-chain of insulin and the B-domain of ILP was completely nonproductive (7). The similar circular dichroism spectra of insulin and double-chain recombinant ILP suggested that the ILP adopted an insulin-like structure (6), so its absence of insulin activity was probably due to the absence of an insulin-receptor-binding patch formed by the side chain of some residues on the ILP surface. We deduced that if the receptor-binding related residues of insulin were grafted onto the corresponding position of ILP, these grafted as well as those inborn insulin-receptor-binding related residues would form an insulin-receptor-binding patch on the ILP surface and then the ILP analogues would acquire mammalian insulin activity. This structure–function-based design also can mimic the natural evolution process of the amphioxus ILP to mammalian insulin in vitro. Therefore, on the basis of successful expression of a single-chain ILP which can be converted to double-chain form by enzymatic cleavage, we prepared six double-chain ILP analogues, [A2Ile]ILP, [B12Val, B16Tyr]-ILP, [B25Phe]ILP, [A2Ile, B12Val, B16Tyr, B25Phe]ILP

<sup>†</sup> This work was supported by grants from the Chinese Academy of Sciences (KJ951-B1-606) and the National Foundation of Nature Science (30170209).

\* Correspondence should be addressed to this author at State Key Laboratory of Molecular Biology, Shanghai Institute of Biochemistry and Cell Biology, SIBS, Chinese Academy of Sciences, 320 Yue-Yang Rd., Shanghai 200031, China. Tel: (86) 021-64374430. Fax: (86) 021-64338357. E-mail: fengym@sunm.shnc.ac.cn.

<sup>1</sup> Abbreviations: IGF-1, insulin-like growth factor 1; IGF-2, insulin-like growth factor 2; BSA, bovine serum albumin; FBS, fetal bovine serum; CT, cholera toxin; Tf, transferrin; EGF, epidermal growth factor; PBS, phosphate-buffered saline; CD, circular dichroism; UV, ultraviolet.



FIGURE 1: Amino acid sequence of human insulin and the recombinant double-chain amphioxus insulin-like peptide (rILP). Asterisks represent the insulin residues related to the insulin–receptor interaction; triangles represent the rILP residues that had been partially or fully replaced by the corresponding residue of insulin.

(four-mutated ILP), [A2Ile, B12Val, B16Tyr, B24Phe, B25Phe]ILP (five-mutated ILP), and [A2Ile, B12Val, B16Tyr, B24Phe, B25Phe, B26Tyr]ILP (six-mutated ILP) (the residues of these ILP analogues were numbered according to those of insulin), by site-directed mutagenesis and measured their structure as well as biological activities. The six residues grafted onto ILP are relevant to the insulin–receptor interaction (8–10). These grafted residues can be divided into two classes: the first class residues are those critical to insulin–receptor interaction, including A2Ile, B12Val, B24Phe, and B25Phe; the second class residues are those with only moderate contribution to insulin–receptor interaction, including B16Tyr and B26Tyr. Together with those inborn insulin–receptor-binding related residues, A1Gly, A3Val, A19Tyr, and B6Leu (11), the multimutated ILP analogue has acquired all of the side chains related to binding with insulin receptor (Figure 1). The evident insulin activity increase of the five- and six-mutated ILP analogues indicated that these grafted and those inborn insulin–receptor-binding related residues on ILP indeed form an insulin–receptor-binding patch; the natural evolution of amphioxus ILP to mammalian insulin is a possible process and can be mimicked in the laboratory. Additionally, the possible different effects of the B-chain/domain of insulin and ILP on their conformation were also discussed.

## MATERIALS AND METHODS

**Materials.** The *Escherichia coli* strains used were DH12S and RZ1032 (dut<sup>−</sup>, ung<sup>−</sup>). *Saccharomyces cerevisiae* XV700-6B (leu2, ura3, pep4) and helper phage R408 were kindly provided by Michael Smith (University of British Columbia, Vancouver, Canada). Plasmid pVT102-U/αMFL-ILP was constructed in our laboratory for secretory expression of the single-chain recombinant ILP in yeast (6). In the recombinant single-chain ILP, the C-terminus of the deduced amphioxus ILP B-domain and the N-terminus of its A-domain were linked together by a tripeptide, Ala-Ala-Lys, and the B29Arg was replaced by Lys for conversion to the double-chain form by endoproteinase Lys-C cleavage. The site-directed mutagenesis oligonucleotide primers were chemically synthesized.

**DNA Manipulation.** The plasmids encoding [A2Ile]ILP, [B12Val, B16Tyr]ILP, [B25Phe]ILP, the four-mutated ILP, the five-mutated ILP, and the six-mutated ILP were constructed using a gapped duplex DNA approach for site-directed mutagenesis (12). The presence of the expected mutations was confirmed by DNA sequencing.

**Expression and Purification of Single-Chain ILP Analogues.** The plasmids encoding the ILP analogues were transformed into *S. cerevisiae* XV700-6B (leu2, ura3, pep4), and the transformed yeast cells were cultured in a 16 L fermenter for 3 days, respectively. The expressed single-

chain ILP analogues were purified from the media in four steps (6). First, the ILP analogue was precipitated from the media supernatant by trichloroacetic acid; second, the precipitate was dissolved with 1 M acetic acid and applied to a Sephadex-G50 column; third, the product was purified by DEAE ion exchange chromatography; fourth, the product was further purified by C8 reverse-phase HPLC. The purity of the ILP analogues was determined by pH 8.3 native polyacrylamide gel electrophoresis (pH 8.3 PAGE) and analytical C8 reverse-phase HPLC. Amino acid composition analysis of the single-chain [A2Ile]ILP was also carried out.

**Conversion of Single-Chain ILP Analogues to Double-Chain Forms.** The purified single-chain ILP analogues were dissolved in 0.1 M NH<sub>4</sub>HCO<sub>3</sub> buffer (pH 8.5). The protein concentration was adjusted to about 10 mg/mL. Then the Lys-C endoproteinase was added to the solution at about a mass ratio of 1:500, and the reaction was carried out at 25 °C overnight. Then, double-chain ILP analogues were purified by C8 reverse-phase HPLC. Their purity was analyzed by native pH 8.3 PAGE. Their molecular mass was measured by electrospray mass spectrometry.

**Circular Dichroism Studies.** The samples were dissolved in 5 mM HCl. The protein concentration was determined by the Lowry method (13). The final concentration of the samples was adjusted to 0.2 mg/mL. Circular dichroism measurements were performed on a Jasco-715 circular dichroism spectropolarimeter. The spectra were recorded at room temperature (250–190 nm for far-UV spectra and 320–245 nm for near-UV spectra). Cell path length was 0.1 and 1.0 cm for far-UV measurement and near-UV measurement, respectively. The data were expressed as molar ellipticity.

**Binding with Human Insulin Receptor.** Receptor binding assay of the double-chain ILP analogues with human insulin receptor was performed using human placental membrane as described previously (14). The membrane insulin receptor (total protein is about 250 μg) was incubated with <sup>125</sup>I-labeled insulin (approximately 10<sup>5</sup> cpm) plus a selected amount of insulin or ILP analogues in a total volume of 0.4 mL containing 50 mM Tris-HCl, 1% BSA, pH 7.5, buffer, at 4 °C overnight. After incubation, the unbound <sup>125</sup>I-labeled insulin was washed away with ice-cold 50 mM Tris-HCl, 0.1% BSA, pH 7.5, buffer 3 times, and the radioactivity of the precipitate was counted. The receptor binding activities of the ILP analogues were calculated from the dosages used for 50% inhibition of <sup>125</sup>I-labeled insulin bound with insulin receptor.

**Growth-Promoting Activity Assay.** The growth-promoting activities of the wild-type double-chain ILP, the five-mutated ILP, and the six-mutated ILP were measured by the GR2H6 cell system as described previously (15). GR2H6 cells were cultured in DME/F12 media containing 10% FBS in 5% CO<sub>2</sub> conditions at 37 °C. GR2H6 cells were seeded onto 96-well plates (10<sup>4</sup> cells/mL) and cultured in DME/F12 media containing 1 mg/mL BSA, 10 ng/mL CT, 10 μg/mL Tf, 10 ng/mL EGF, and different concentration of the samples. After 58 h, the cells were fixed and stained with crystal violet buffer (0.02% crystal violet, 0.2 M PBS, pH 6.8) and then dissolved with 200 μL of 10% acetic acid, and the absorbance was measured at 590 nm.

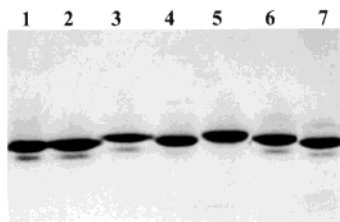


FIGURE 2: Native pH 8.3 PAGE analysis of the six double-chain ILP analogues. Lanes 1–7 are wild-type ILP, [A2Ile]ILP, [B12Val, B16Tyr]ILP, [B25Phe]ILP, the four-mutated ILP, the five-mutated ILP, and the six-mutated ILP, respectively.

Table 1: Molecular Masses of the Six Double-Chain ILP Analogues Measured by Electrospray Mass Spectrometry

samples	measured values	theoretical values
[A2Ile] ILP	5449.0	5450.0
[B12Val, B16Tyr] ILP	5553.0	5554.2
[B25Phe] ILP	5482.0	5483.1
four-mutated ILP	5587.0	5587.3
five-mutated ILP	5570.5	5571.3
six-mutated ILP	5647.1	5647.4

## RESULTS

**Site-Directed Mutagenesis.** The expected mutations on the recombinant ILP gene were confirmed by DNA sequencing (data not shown). The expression vectors were designated as pVT102-U/ $\alpha$ -MFL-[A2Ile]ILP, pVT102-U/ $\alpha$ -MFL-[B12Val, B16Tyr]ILP, pVT102-U/ $\alpha$ -MFL-[B25Phe]ILP, pVT102-U/ $\alpha$ -MFL-[A2Ile, B12Val, B16Tyr, B25Phe]ILP, pVT102-U/ $\alpha$ -MFL-[A2Ile, B12Val, B16Tyr, B24Phe, B25Phe]ILP, and pVT102-U/ $\alpha$ -MFL-[A2Ile, B12Val, B16Tyr, B24Phe, B25Phe, B26Tyr]ILP.

**Expression, Purification, and Conversion of Single-Chain ILP Analogues to Double-Chain Forms.** The expression vectors of the six ILP analogues were transformed into yeast cells. After fermentation and purification, the single-chain recombinant ILP analogues were obtained and then converted to double-chain forms by endoproteinase Lys-C cleavage. The molecular mass of the six double-chain ILP analogues was measured by electrospray mass spectrometry as listed in Table 1. The measured molecular masses of the six analogues are consistent with the expected values. The result of the amino acid composition analysis of the single-chain [A2Ile]ILP was also the expected values: Ile 0.85(1), Leu 4.26(4). The purity of the double-chain ILP analogues was analyzed by the native pH 8.3 PAGE as shown in Figure 2. The six ILP analogues were homogeneous as judged by PAGE.

**Circular Dichroism Analysis.** The structural changes of the six double-chain ILP analogues were analyzed by circular dichroism compared with the wild-type double-chain ILP as shown in Figure 3. The near-UV spectra difference between the six-mutated ILP and the other analogues in the aromatic region was caused by the introduction of a B26Tyr residue, which indicated that the side chain of the B26Tyr is in an asymmetrical microenvironment resulting from the three-dimensional structure of the molecule. The similarity of the near-UV and far-UV spectra between the analogues and the wild-type ILP indicated that the residues' replacement did not cause significant structural disturbance on the ILP molecule.

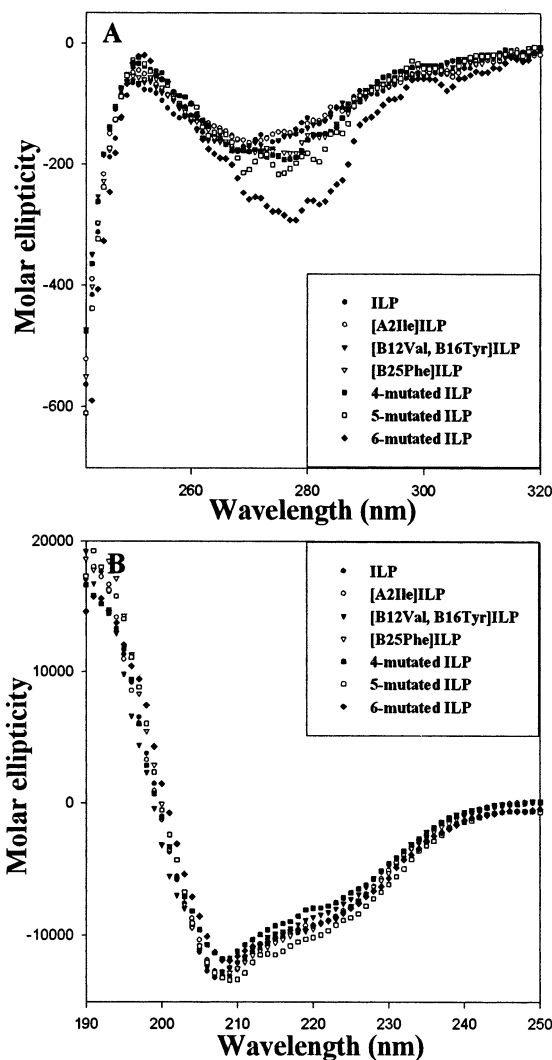


FIGURE 3: Circular dichroism analysis of the six double-chain ILP analogues. (A) Near-UV spectra; (B) far-UV spectra.

**Binding with Human Insulin Receptor.** The insulin-receptor-binding activity of the six double-chain ILP analogues was measured and compared with that of the native porcine insulin as shown in Figure 4. The relative insulin-receptor-binding activity calculated from the dosages used for 50% inhibition of  $^{125}$ I-insulin bound with insulin receptor of the four-, five-, and six-mutated ILP was 0.14%, 11%, and 11% of porcine insulin, respectively, while the other three analogues acquired no detectable insulin-receptor-binding activity.

**Growth-Promoting Activity Assay.** Except for the function of metabolic regulation, insulin also has growth-promoting potency. Here we measured the growth-promoting activity of the double-chain wild-type ILP, the five-mutated ILP, and the six-mutated ILP using the GR2H6 cell system (15) as shown in Figure 5. Their relative activities compared with that of insulin or IGF-1 calculated from the ED<sub>50</sub> values are listed in Table 2. The growth-promoting activity of the five- and six-mutated ILP analogues was both about 50% of insulin while that of the wild-type ILP was not detectable.

## DISCUSSION

Based on the structure–function design, we converted the completely inactive amphioxus ILP to a molecule with



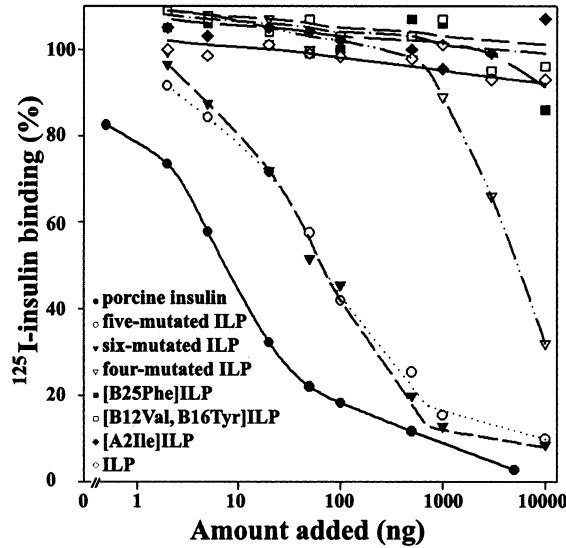


FIGURE 4: Insulin-receptor-binding activity of the six double-chain ILP analogues.

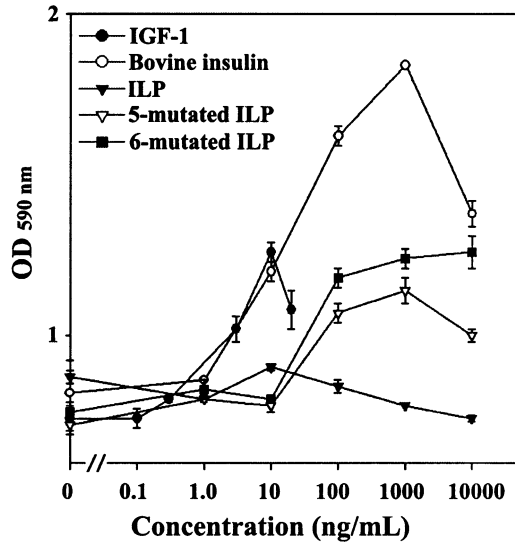


FIGURE 5: Growth-promoting activity of the wild-type double-chain ILP, the five-mutated ILP, and the six-mutated ILP measured by the GR2H6 cell system.

Table 2: Relative Growth-Promoting Activity of the Double-Chain Five- and Six-Mutated ILP Measured by the GR2H6 Cell System<sup>a</sup>

samples:	IGF-1	bovine insulin	five-mutated ILP	six-mutated ILP
ED <sub>50</sub> (ng/mL)	2.3	17.8	35.5	37.6
% of insulin	770	100	50	47
% of IGF-1	100	13	6	6

<sup>a</sup> The activity of wild-type ILP was not detectable.

moderate mammalian insulin activities. The significant increase of the insulin activities of the five- and six-mutated ILP analogues indicated the following: first, these grafted and those inborn insulin-receptor-binding related residues of the ILP analogues indeed form a functional patch similar to the receptor-binding patch formed on the insulin surface; second, the substitution resulted in little disturbance on the structure of ILP, so ILP can be used as a scaffold molecule to investigate the role of the insulin residues.

The six residues introduced into the ILP molecule can be divided into two classes. The first class is the residues that

are critical for insulin–receptor interaction, including A2Ile, B12Val, B24Phe, and B25Phe. The second class is the residues that are not critical but contribute moderately to the insulin–receptor interaction, including B16Tyr and B26Tyr. To obtain the ILP analogue with the insulin activity as high as possible, the second class residues were also introduced into the present ILP analogues. Although B16Tyr and B26Tyr are not critical for insulin–receptor interaction, they are usually included in the receptor-binding surface (1, 8) in the proposed insulin–receptor interaction model. The replacements of B26Tyr usually cause a moderate decrease of the insulin activity although the despentapeptide insulin with amide C-terminal B-chain retained full insulin activity (16). The present results showed that B26Tyr did not significantly contribute to the insulin–receptor interaction in the ILP analogues since the five- and six-mutated ILP acquired similar insulin activity. The insulin-receptor-binding activity of the five-mutated ILP is about 80-fold higher than that of the four-mutated ILP. The activity discrepancy reflects the crucial role of the side chain B24Phe residue in insulin–receptor interaction, which is also consistent with the result of insulin mutational analysis (17). The [B24Tyr, B26Phe]-insulin retained only 2% receptor-binding activity; that is, the Tyr replacement on the B24 position caused about a 50-fold decrease of insulin activity (17). So the insulin activity decrease caused by the Tyr substitution on the position of B24 in insulin and in ILP analogues is at the same level. The present result from ILP mutational analysis can provide more information about the insulin receptor-binding surface although it had been extensively investigated on insulin itself.

By the replacement of only several residues, a molecule with new function was created from a fully inactive parent molecule, which showed the power of the structure–function-based design. If this new molecule were created by random mutation, the trials would be an astronomical number. The present study was also an in vitro evolution process; that is, a new molecule was created through mutations that accelerated the natural evolution progress and made it possible to mimic in the laboratory. The natural evolution created all kinds of protein molecules with different biological functions, but the natural evolution progress was very slow. By the structure–function-based design, the molecules with new function can be created quickly in laboratory. The evident increase of the insulin activity of the five- and six-mutated ILP implied that the natural evolution of amphioxus ILP to mammalian insulin was a possible process. We could deduce that some residues of ILP mutated spontaneously and randomly in the long evolution process and then the mammalian insulin gradually emerged by natural selection.

Although the five- and six-mutated ILP had already obtained all of the critical side chains for binding with mammalian insulin receptor, the ILP analogues did not acquire full insulin activities. Considering the fact that the hybrid Ins(B)/ILP(A) had 5% insulin activity (7), moreover, the replacement of A2Leu by Ile led to a fully active hybrid; we deduced that there would be subtle difference between the conformation of the insulin-receptor-binding patch formed on the ILP surface and that formed on the insulin surface. Furthermore, we deduced that the subtle conformational difference is more possibly manipulated by their B-chain/domain sequence. In a previous report, the recom-

bination of the separate A-chain of insulin and B-domain of ILP was completely nonproductive while the recombination of the separate A-domain of ILP and the B-chain of insulin was efficient, which was possibly caused by the different conformation of their B-chain/domains (7). The insulin-like three-dimensional structure is mainly composed of three  $\alpha$ -helical segments (A2–A8, A13–A19, and B9–B19 in insulin) (18–21) stabilized by three disulfides (one intrachain bond, A6–A11; two interchain bonds, A7–B7 and A20–B19) (22–26). Although its three-dimensional structure had not been solved, we can presume that the ILP adopts a reasonably close insulin-like structure. In the insulin-like structure, the B-chain/domain encodes the largest  $\alpha$ -helical segment that is more stable than the other two  $\alpha$ -helical segments (22–26). So the conformation of the B-chain/domain is more important for manipulating the conformation of the whole molecule. The different sequences of the B-chain/domain of insulin and the multimutated ILP probably resulted in a little different conformation, so the insulin-receptor-binding patch formed on insulin and that formed on the ILP analogues had different effectiveness for binding with insulin receptor.

The double-chain ILP is completely inactive with mammalian insulin receptor, but there are receptors which preferentially bind with the double-chain ILP in amphioxus (27). So ILP is a functional protein in amphioxus, and its structure and the receptor-binding patch are suitable with the structure of its receptor. The most critical aspect of the evolution of ILP is the evolution of its receptor-binding patch. This progress is coevolved with the evolution of its receptor. Until now we had no knowledge about the receptor-binding surface of ILP. The present ILP analogues provide good materials for investigating the receptor-binding surface of ILP in later research.

## REFERENCES

- Murray-Rust, J., Mcleod, A. N., Blundell, T. L., and Wood, S. P. (1992) *BioEssays* 14, 325–331.
- Humbel, R. E. (1990) *Eur. J. Biochem.* 190, 445–462.
- Cook, R. M., Harvey, T. S., and Campbell, I. D. (1991) *Biochemistry* 30, 5484–5491.
- Chan, S. J., Cao, Q. P., and Steiner, F. D. (1990) *Proc. Natl. Acad. Sci. U.S.A.* 87, 9319–9323.
- Chu, Y. C., Hu, S. Q., Zong, L., Burke, G. T., Gammeltoft, S., Chan, S. J., Steiner, D. F., and Katsoyannis, P. G. (1994) *Biochemistry* 33, 11278–11285.
- Shen, L., Guo, Z.-Y., Chen, Y., Liu, L.-Y., and Feng, Y.-M. (2001) *Acta Biochim. Biophys. Sin.* 33, 629–633.
- Chu, Y.-C., Burke, T., Gammeltoft, S., Chan, S. J., Steiner, D. F., and Katsoyannis, P. G. (1994) *Biochemistry* 33, 13087–13092.
- Schaffer, L. (1994) *Eur. J. Biochem.* 221, 1127–1132.
- Kristensen, C., Kjeldsen, T., Wiberg, F. C., Schaffer, L., Hach, M., Havelund, S., Bass, J., Steiner, D. F., and Andersen, A. S. (1997) *J. Biol. Chem.* 272, 12978–12983.
- Chen, H., Shi, M., Guo, Z.-Y., Tang, Y.-H., Qiao, Z.-S., Liang, Z.-H., and Feng, Y.-M. (2000) *Protein Eng.* 13, 779–782.
- Nakagawa, S. H., and Tager, H. S. (1991) *J. Biol. Chem.* 266, 1150–11509.
- Kramer, W., Drusta, V., Jansen, H. W., Kramer, B., Pflugfelder, M., and Fritz, H. J. (1984) *Nucleic Acid Res.* 12, 9441–9454.
- Lowrey, O. H., Rosebrough, N. O., Farr, A. L., and Randall, R. (1951) *J. Biol. Chem.* 193, 265–275.
- Feng, Y.-M., Zhu, J.-H., Zhang, X.-T., and Zhang, Y.-S. (1982) *Acta Biochim. Biophys. Sin.* 14, 137–143.
- Ma, J.-G., Li, M.-Y., Zheng, J.-M., Cui, D.-F., Feng, Y.-M., and Jing, N.-H. (1999) *Acta Biochim. Biophys. Sin.* 31, 274–278.
- Nakagawa, S. H., and Tager, H. S. (1986) *J. Biol. Chem.* 261, 7332–7341.
- Mirmira, R. G., Nakarawa, S. H., and Tager, H. S. (1991) *J. Biol. Chem.* 266, 1428–1436.
- Baker, E. N., Blundell, T. L., Cutfield, J. F., Cutfield, S. M., Dodson, E. J., Dodson, G. G., Hodgkin, D. M. C., Hubbard, R. E., Isaacs, N. W., Reynolds, C. D., Sakabe, K., Sakabe, N., and Vijayan, N. M. (1988) *Philos. Trans. R. Soc. London, Ser. B* B319, 369–456.
- The Peking Insulin Structure Research Group (1974) *Sci. Sin.* 17, 752–778.
- Weiss, M. A., Hua, Q.-X., Frank, B. H., Lynch, C., and Shoelson, S. E. (1991) *Biochemistry* 30, 7373–7389.
- Roy, M., Lee, R. W.-K., Brange, J., and Dunn, M. F. (1990) *J. Biol. Chem.* 265, 5448–5453.
- Hua, Q.-X., Hu, S.-Q., Frank, B. H., Jia, W., Chu, Y.-C., Wang, S.-H., Burke, G. T., Katsoyannis, P. G., and Weiss, M. A. (1996) *J. Mol. Biol.* 264, 390–403.
- Hua, Q.-X., Narhi, L., Jia, W., Arakawa, T., Rosenfeld, R., Hawkins, N., Miller, J. A., and Weiss, M. A. (1996) *J. Mol. Biol.* 259, 297–313.
- Guo, Z.-Y., and Feng, Y.-M. (2001) *Biol. Chem.* 382, 443–448.
- Weiss, M. A., Hua, Q.-X., Jia, W., Chu, Y.-C., Wang, R.-Y., and Katsoyannis, P. G. (2000) *Biochemistry* 39, 15429–15440.
- Hua, Q.-X., Nakagawa, S. H., Jia, W., Hu, S.-Q., Chu, Y.-C., Katsoyannis, P. G., and Weiss, M. A. (2001) *Biochemistry* 40, 12299–12311.
- Pashmforoush, M., Chan, S. J., and Steiner, D. F. (1996) *Mol. Endocrinol.* 10, 857–866.

BI020223X